

Trapping of waves and null geodesics for rotating black holes

S. Dyatlov¹ and M. Zworski²

¹*Department of Mathematics, Massachusetts Institute of Technology, Cambridge, MA 02139, USA*

²*Department of Mathematics, University of California, Berkeley, CA 94720, USA*

(Dated: October 15, 2013)

We present dynamical properties of linear waves and null geodesics valid for Kerr and Kerr–de Sitter black holes and their stationary perturbations. The two are intimately linked by the geometric optics approximation. For the nullgeodesic flow the key property is the *r-normal hyperbolicity* of the trapped set and for linear waves it is the distribution of quasi-normal modes: the exact quantization conditions do not hold for perturbations but the bounds on decay rates and the statistics of frequencies are still valid.

PACS numbers: 04.70.Bw, 03.65.Nk, 42.25.Bs, 25.70.Ef, 05.45.-a

Keywords: Black holes, quasi-normal modes

The Kerr solutions [1] to Einstein equations are considered as physically relevant models of rotating black holes. The Kerr metrics depend on two parameters: mass M and rotational parameter a ; the special case $a = 0$ is the Schwarzschild metric. The *Kerr-de Sitter* solutions describe rotating black holes in the case of positive cosmological constant, $\Lambda > 0$ – see (1) below for the formula for the metric and Fig. 1 for the plot of admissible values of the parameters. Due to the observed *cosmic acceleration* [2], the current cosmological Λ CDM model assumes $\Lambda > 0$. As explained below, $\Lambda > 0$ makes the study of the topic of this article, *quasi-normal modes* for black holes (QNM), mathematically more tractable while not affecting the description of the physical phenomenon of ringdown [3].

The classical dynamics of Kerr black holes is concerned with the behavior of null geodesics of the corresponding metric, that is, the trajectories of photons in the gravitation field of the black hole. The key dynamical object is the *trapped set*, consisting of all null geodesics in phase space (position and momentum space) which never cross the event horizon of the black hole or escape to infinity. In other words, this is the set where the strength of gravitational fields forces photons to travel on bounded orbits.

In case of Schwarzschild black hole ($a = 0$) the time slice of the trapped set is just the phase space of a sphere (mathematically, the cotangent bundle of a sphere) called the *photon sphere*: along the photon sphere, all photons travel on closed orbits. A traveller who crosses the photon sphere, although still visible to outsiders, is forced to cross the black hole horizon eventually. In the case of nonzero angular momentum ($a \neq 0$) the trapped set is no longer the phase space/cotangent bundle of a smooth spatial set; instead it becomes a non-trivial object in the phase space. The photons are *trapped* because of the strength of the gravitational field but most of them (that is, a set of full measure) no longer travel along closed orbits – see Fig. 2 for a visualization of the trapped set and (2) for the analytic description. Although the trapped set is no longer the phase space of a spatial object, it remains a smooth five dimensional manifold. The sym-

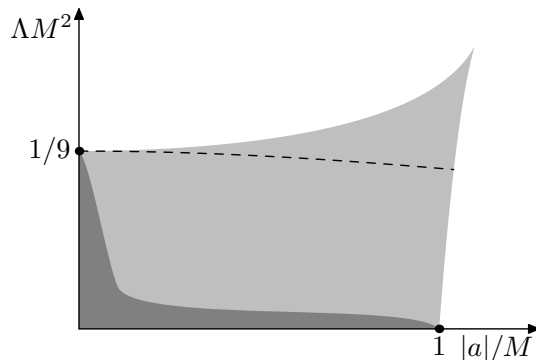


FIG. 1. Numerically computed admissible range of parameters for the subextremal Kerr–de Sitter black hole (light shaded) [30] and the range to which our results apply (dark shaded). QNM are defined and discrete for parameters below the dashed line, $(1 - \alpha)^3 = 9\Lambda M^2$, see [8, §3.2].

plectic form on the phase space of a time slice (see (3)) restricts to a non-degenerate form on the trapped set. That means that the time slice of the trapped set is a smooth symplectic manifold.

A remarkable feature of the geodesic flow on Kerr(–de Sitter) metrics is its complete integrability [4] in the sense of Liouville-Arnold [5]: there exist action variables which define invariant tori on which the motion is linear.

In this article we describe another important feature of the dynamics: *r-normal hyperbolicity*. It means that the flow is hyperbolic in directions normal to the trapped set – see (4) for a mathematical definition. This property, unlike complete integrability, is known to be stable under perturbations [6]: a small C^r (r times differentiable) stationary perturbation of the metric will destroy complete integrability but will preserve C^r structure of the trapped set and *r-normal hyperbolicity*. For Kerr black holes the condition holds for *each* r and hence regular perturbations will maintain the regular structure of the trapped set of light trajectories [7, 8].

The classical dynamical features are crucial for the behavior of gravitational waves emitted by black holes, es-

pecially during the *ringdown* phase, when a black hole spacetime settles down after a large cosmic event such as a binary black hole merger. Gravitational waves are expected to be observable by the existing detectors, once they are running at full capacity, and to provide information about the parameters of astrophysical black holes. During the ringdown phase, the behavior of gravitational waves is driven by the linearized system [3] and is much simpler to simulate numerically than the merger phase [9–11]. At ringdown, gravitational waves have a fixed set of complex frequencies, known as *quasi-normal modes (QNM)* [3] and depending only on the parameters of the black hole, rather than the specifics of the event. The simplest model of ringdown is obtained by solving the linear scalar wave equation for the Kerr(–de Sitter) black hole spacetimes, and in that case quasi-normal modes can be rigorously defined. More complicated linearizations have also been studied [3, 12] but we concentrate on the simplest setting here. On the relevant time and space length scales, the value of the cosmological constant Λ does not have a physical effect on the ringdown since gravitational waves are generated in a neighborhood of the black hole but $\Lambda > 0$ makes the mathematical definition of QNM much easier by eliminating the polynomial fall-off for waves [3, §5.1].

In a more general physical or geometric context of scattering theory, quasi-normal modes, also known as resonances, replace bound states (eigenvalues), for systems which allow escape of energy [13] and simultaneously describe oscillations (real parts of the mode) and decay (imaginary parts). They appear in expansions of waves – see (6) below, just as waves in bounded regions are expanded using eigenvalues. This dynamical interpretation immediately suggests that the distribution of QNM is related to the trapping on the classical level – see [14, 15] for a discussion and recent experimental results in the setting of microwave billiards.

The relation between dynamics and distribution of QNM/resonances has been particularly well studied in problems where a reduction to one dimension is possible. More generally, complete integrability allows quantization rules which can be used to describe resonances in the semiclassical/high energy limit. In the setting of black holes this goes back to [16].

For Schwarzschild black holes the Regge–Wheeler reduction (see (7) below) produces a one dimensional potential similar to the Eckart barrier potential $\cosh^{-2} x$ for which resonances are given by $\pm\sqrt{3}/2 - i(n+1/2)$ – see [17] for a review in the context of chemistry, [18] for a mathematical discussion in the Schwarzschild case, and [19] for a general study of Pöschl–Teller potentials. Putting together different angular momenta produces an (approximate) lattice of resonances.

When $a \neq 0$, that is, in the genuine Kerr case, the degenerate QNM split in a way similar to the Zeeman effect. They have been recently studied using WKB methods based on the completely integrable structure [20–23] and the Zeeman-like splitting has been rigorously confirmed.

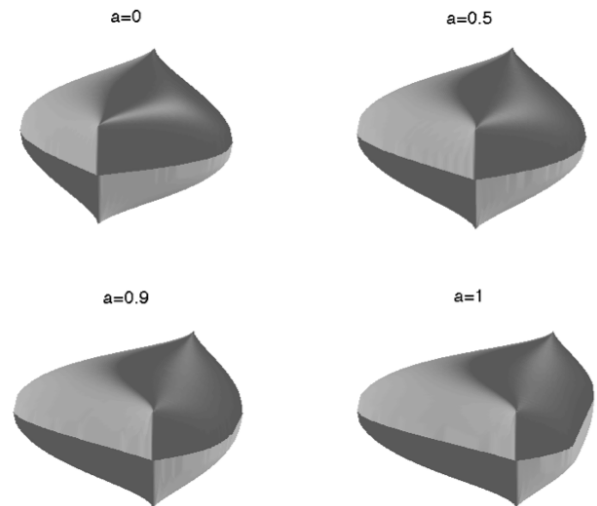


FIG. 2. Visualization of the trapped set for different values of a , with $\Lambda = 0$. The figures show the four-dimensional set $K \cap \{\xi_t = 1\}$ (K is the five dimensional trapped set) projected to the coordinates $(x, y, z) = (\xi_\varphi, \theta, \xi_\theta)$. For $a = 0$ this corresponds to the visualization of the phase space of the 2-sphere: the sphere is parametrized by the coordinates $0 \leq \theta \leq \pi$, $0 \leq \varphi < 2\pi$, $(\sin \theta \cos \varphi, \sin \theta \sin \varphi, \cos \theta)$. The conjugate coordinates are denoted ξ_θ and ξ_φ and the restriction to $\xi_t = 1$ means that $\xi_\theta^2 + \sin^{-2} \theta \xi_\varphi^2 = 27M^2$. The vertical singular interval in front corresponds to $\theta = 0$, with the symmetrical interval in the back corresponding to $\theta = \pi$: the coordinates (θ, φ) on the sphere are singular at that point. The structure of K becomes more interesting when $a > 0$ as shown in the three examples. The additional coordinate, not shown in the figures, r is a function of ξ_φ and ξ_t only. When $a = 0$, we have $r = 3M$, but r gets larger to the left ($\xi_\varphi > 0$) and smaller to the right ($\xi_\varphi < 0$) when $a > 0$. When $a = 1$ we see the flattening in the (θ, ξ_θ) -plane at extremal values of ξ_φ : the trapped set touches the event horizon $r = 1$ which results in lack of decay, and some QNM have null imaginary parts [22, 23]. Dynamically and invariantly this corresponds to the vanishing expansion rates – see Fig. 4.

The point of this article is to describe recent mathematical results [7, 8, 18, 20, 21, 24, 25] which apply to *stationary perturbations of Kerr metrics* and do not depend on the completely integrable structure. They are based on the use of the r -normal hyperbolicity of the trapped set and show that many features of QNM studied using WKB methods available in the completely integrable case persist for perturbations. The r -normal hyperbolicity of black hole dynamics [7] has not been discussed in the physics literature but the importance of normal hyperbolicity in molecular dynamics has been explored [26]. It would be interesting to consider the stability of r -normally hyperbolic dynamics under more general, non-stationary, perturbations.

In particular, we show how dynamical features (such as the maximal and minimal expansion rates) and statistical properties of the distribution of quasi-normal modes (QNM) depend on $a = J/Mc$, the rescaled angular mo-

mentum. For the exact Kerr (or Kerr–de Sitter) black hole the counting law for QNM and their maximal and minimal decay rates determine the mass and the angular momentum. For the perturbed case, they determine stable features such as the symplectic volume of the trapped set and classical decay rates.

The presentation is organized as follows: in §II we discuss classical dynamics and define r -normal hyperbolicity in a precise way; in §III we describe the challenges of rigorously defining of QNM for Kerr and Kerr–de Sitter black holes. The difficulties come from the presence of the ergosphere which obstruct standard methods for defining resonances (lack of coercivity/ellipticity of the stationary wave equation) and from the “size” of infinity in the Kerr ($\Lambda = 0$) case. In §IV we present the quantitative results about the distribution of QNM valid for perturbations of Kerr black hole: bounds on imaginary parts of the modes (11), the counting law (12), and the consequences for solutions of the wave equation (13). The strongest results are subject to a pinching condition (10) which is valid for all but rapidly rotating rotating black holes. The results presented here and some of the figures have appeared in works aimed at the mathematical audience [8] and this is an attempt to relate them to an active field of research in physics.

II. THE TRAPPED SET OF NULL GEODESICS

We are interested in null geodesics and the wave equation $\square_g u = 0$, where g is the Kerr(–de Sitter) metric [1, 4, 7, 8]. The Kerr–de Sitter metric is a generalization of Kerr to the case of a positive cosmological constant Λ . For a black hole of mass $M > 0$ (for $\Lambda > 0$ there is no unique definition of global mass; here we treat M simply as a parameter of the metric), rotating with speed a the space slice is

$$X = (r_+, r_C) \times \mathbb{S}^2,$$

where $r_C < \infty$ when $\Lambda > 0$, and $r_C = \infty$ when $\Lambda = 0$. The behavior of \square_g for r near r_C is dramatically different in the two cases: for $\Lambda > 0$ the metric is asymptotically hyperbolic in the sense of non-Euclidean geometry (infinity is *large* in the sense that the volume of balls grows exponentially in radius) and for $\Lambda = 0$ it is asymptotically Euclidean (infinity is *small* in the sense that volume of balls grows polynomially). For solutions to the wave equation that produces differences in long time decay and in the behavior at low energies [27–29]. The surface $r = r_+$ is the event horizon of the black hole. When $\Lambda > 0$, $r = r_C$ is the cosmological horizon. While the two horizons have different physical interpretations, their mathematical roles in the study of wave decay and QNM are remarkably similar.

The geodesic flow can be considered as a flow on the phase space (the position-momentum space) of $\mathbb{R} \times X$, that in mathematical terms on the cotangent bundle $T^*(\mathbb{R} \times X)$. We denote the coordinates on $\mathbb{R} \times X$ by

(t, r, θ, φ) (see Fig. 2), and write $(\xi_t, \xi_r, \xi_\theta, \xi_\varphi)$ for the corresponding conjugate (momentum) variables. The flow is given by the classical Hamiltonian flow [5] for the Hamiltonian G ,

$$\begin{aligned} \dot{t} &= \partial_{\xi_t} G, & \dot{r} &= \partial_{\xi_r} G, & \dot{\theta} &= \partial_{\xi_\theta} G, & \dot{\varphi} &= \partial_{\xi_\varphi} G, \\ \dot{\xi}_t &= -\partial_t G, & \dot{\xi}_r &= -\partial_r G, & \dot{\xi}_\theta &= -\partial_\theta G, & \dot{\xi}_\varphi &= -\partial_\varphi G, \end{aligned}$$

where

$$\begin{aligned} G &= \rho^{-2}(G_r + G_\theta), & \rho^2 &= r^2 + a^2 \cos^2 \theta, \\ G_r &= \Delta_r \xi_r^2 - \frac{(1 + \alpha)^2}{\Delta_r} ((r^2 + a^2)\xi_t + a\xi_\varphi)^2, \\ G_\theta &= \Delta_\theta \xi_\theta^2 + \frac{(1 + \alpha)^2}{\Delta_\theta \sin^2 \theta} (a \sin^2 \theta \xi_t + \xi_\varphi)^2, & \alpha &= \frac{\Lambda a^2}{3}. \\ \Delta_r &= (r^2 + a^2) \left(1 - \frac{\Lambda r^2}{3}\right) - 2Mr, & \Delta_\theta &= 1 + \alpha \cos^2 \theta. \end{aligned} \tag{1}$$

The function G is the dual metric to the semi-Riemannian Kerr(–de Sitter) metric g (see for example [8, §3.1] for the formulas for g). It is also the principal symbol of \square_g in the sense that

$$\square_g = G(t, r, \theta, \varphi, \partial_t/i, \partial_r/i, \partial_\theta/i, \partial_\varphi/i), \quad i = \sqrt{-1},$$

modulo a first order differential operator. The limiting radii r_+, r_C solve $\Delta_r = 0$.

The trapped set consists of null geodesics that stay away from $r = r_+, r = r_C$ for all times. The variables (θ, ξ_θ) evolve according to the Hamiltonian flow of G_θ , and ξ_t, ξ_φ are conserved. The trapping depends on the evolution of (r, ξ_r) according to the flow of G_r , which is essentially the one dimensional motion for a barrier top potential [18]. Under the assumptions that either $a = 0$, $9\Lambda M^2 < 1$ or $\Lambda = 0$, $|a| < M$, and for nearby values of M, Λ, a [8, Prop.3.2],[30] the trapped set K is given by

$$K = \{G = 0, \xi_r = 0, \partial_r G_r = 0, \xi \neq 0\}. \tag{2}$$

For $a = 0$, $\partial_r G_r = 0$ gives $r = 3M$, the radius of the photon sphere. For $a \neq 0$, a more careful analysis is required, but K is still a smooth submanifold of the characteristic set $\{G = 0\}$. Moreover, it is symplectic in the sense that the spatial symplectic form σ ,

$$\sigma = d\xi_r \wedge dr + d\xi_\theta \wedge d\theta + d\xi_\varphi \wedge d\varphi, \tag{3}$$

is nondegenerate on the surfaces $K \cap \{t = \text{const}\}$.

Let $\mathcal{C}_+ \subset \{G = 0\}$ be the positive light cone and

$$\varphi^t : \mathcal{C}_+ \rightarrow \mathcal{C}_+$$

the geodesic flow parametrized by t . The r -normal hyperbolicity condition asserts the existence of a C^r (r -times differentiable) splitting

$$T_K \mathcal{C}_+ = TK \oplus \mathcal{V}_+ \oplus \mathcal{V}_-,$$

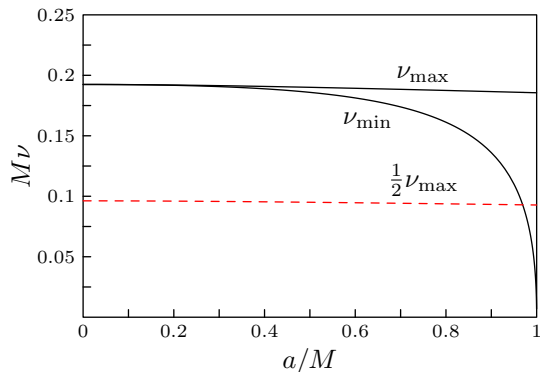


FIG. 3. The dependence of ν_{\max} and ν_{\min} on the parameters M and a in the case of $\Lambda = 0$. The dashed line indicates the range of validity of the pinching condition needed for the Weyl law (12).

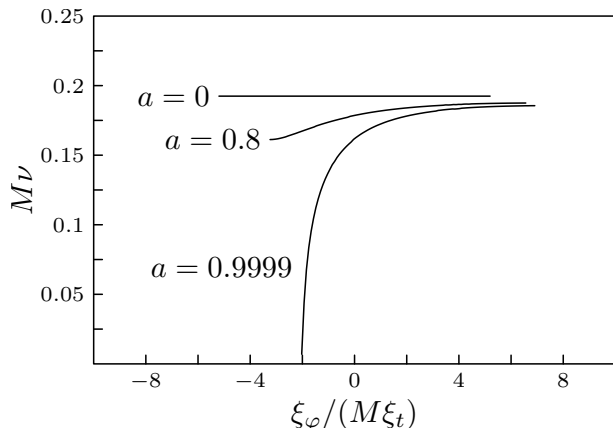


FIG. 4. The pointwise expansion rates ν on Liouville tori $\xi_\varphi/(M\xi_t) = \text{const}$, for $\theta = \pi/2$. When a approaches 1, $\nu = 0$ for some values of ξ_φ which shows that there is no gap and QNM can be arbitrarily close the real axis [22, 23].

invariant under the flow and such that for some constants $\nu > 0, C > 0$,

$$\begin{aligned} \sup_{(x,\xi) \in K} |d\varphi^{\mp t}|_{\mathcal{V}_\pm} &\leq C e^{-\nu t}, \\ \sup_{(x,\xi) \in K} |d\varphi^{\pm t}|_{TK} &\leq C e^{\nu|t|/r}, \quad t \geq 0. \end{aligned} \quad (4)$$

This means that the maximal expansion rates (Lyapunov exponents) on the trapped set are r -fold dominated by the expansion and contraction rates in the directions transversal to the trapped set. As shown in [6],[24, §5.2] r -normal hyperbolicity is stable under perturbations: when G_ϵ is a time independent (that is, stationary) Hamiltonian such that G_ϵ is close to G in C^r near K , the flow for G_ϵ is r -normally hyperbolic in the sense that the trapped set K_ϵ has C^r regularity, is symplectic and (4) holds. For Kerr(-de Sitter) metrics the flow is r -normally hyperbolic for all r as shown in [7, 8, 25], essentially because the flow on K is completely integrable.

Key dynamical quantities are the minimal and maxi-

mal expansion rates $0 < \nu_{\min} \leq \nu_{\max}$, characterized by inequalities true for all $\epsilon > 0$, a constant C_ϵ depending on ϵ ,

$$C_\epsilon^{-1} e^{-(\nu_{\max} + \epsilon)t} \leq |d\varphi^t|_{\mathcal{V}_-} \leq C_\epsilon e^{-(\nu_{\min} - \epsilon)t},$$

$t > 0$. For Kerr(-de Sitter) metrics, the quantities ν_{\min}, ν_{\max} are obtained by taking the minimum and maximum of averages of the local expansion rate

$$\nu = \sqrt{-2\Delta_r \partial_r^2 G / |\partial_{\xi_t} G|},$$

on the Liouville tori [5] of the flow of G_θ on the trapped set.

III. DEFINITION AND DISCRETENESS OF QUASI-NORMAL MODES

The *scattering resonances*, called *quasi-normal modes* (QNM) in the context of black holes [12], replace eigenmodes when one switches from closed systems to open systems – see [14] for a recent experimental discussion. They are the frequencies ω of oscillating solutions to the wave equation

$$\square_g(e^{-i\omega t} v(r, \theta, \varphi)) = 0, \quad (5)$$

which continue smoothly across the event horizons.

Solutions to $\square_g u = 0$ are expected to have expansions

$$u(t, r, \theta, \varphi) \sim \sum_k e^{-it\omega_k} u_k(r, \theta, \varphi) \quad (6)$$

valid in a suitable sense [21, 31]. The fact that QNM ω_k form a discrete set in the lower half-plane is nontrivial but it is now rigorously known in the case of Kerr-de Sitter and its perturbations [18, 20, 25, 31, 32].

In the simpler Schwarzschild-de Sitter case we indicate the reason for discreteness of the set of QNM as follows. The equation (5) can be rewritten as $P(\omega)v = 0$, where $P(\omega)$ is obtained from $-\rho^2 \square_g$ by replacing ∂_t with $-i\omega$. The operator $P(\omega)$ is spherically symmetric; its restriction to the space of spherical harmonics with eigenvalue $\ell(\ell + 1)$, written in the Regge-Wheeler coordinate x [20, §4], is the Schrödinger operator

$$P_\ell(\omega) = -\partial_x^2 + \omega^2 V_1(x) + \ell(\ell + 1)V_2(x), \quad (7)$$

where the potentials V_1 and V_2 are real analytic (their Taylor series converge to their values) and satisfy

$$V_1(x) = -V_\pm^2 + \mathcal{O}(e^{-A_\pm|x|}), \quad V_2(x) = \mathcal{O}(e^{-A_\pm|x|}),$$

as $x \rightarrow \pm\infty$; here $A_\pm > 0$, $V_- = r_-^2$, $V_+ = r_+^2$. (When $\Lambda = 0$ then $V_2 \sim x^{-2}$ as $x \rightarrow +\infty$ and that creates problems at low energies [27, 28]. More precisely, it is expected that due to the slow decay of the potential, the resolvent is not holomorphic in a neighborhood of zero and even in simplest cases such as Schwarzschild, there

is no mathematical argument excluding the possibility of accumulation of QNM at zero.) A number $\omega \in \mathbb{C}$ is a QNM if there exists an angular momentum ℓ and a nonzero solution $v(x)$ to the equation $P_\ell(\omega)v = 0$ satisfying the outgoing condition: near $x = \pm\infty$, $e^{\mp iV_\pm \omega x} v(x)$ is a smooth function of $e^{-A_\pm |x|}$. The outgoing condition follows naturally from the requirement that $e^{-i\omega t} v(x)$ extends smoothly past the event horizon of the black hole. For fixed ℓ , it follows by standard one-dimensional methods that the set of all corresponding ω is discrete.

Showing that as $\ell \rightarrow \infty$, quasi-normal modes corresponding to different values of ℓ do not accumulate is more delicate: we need to know that if $|\omega| \leq R$ and ℓ is large enough depending on R , then ω cannot be a QNM corresponding to ℓ . Assume the contrary and let $v(x)$ be the corresponding solution to the equation $P_\ell(\omega)v = 0$. We fix large $X > 0$ independently of ℓ , to be chosen later. The potential V_2 is everywhere positive, therefore for ℓ large enough depending on R, X , $\text{Re}(\omega^2 V_1(x) + \ell(\ell+1)V_2(x)) > 0$ for $x \in [-X, X]$. If v satisfied a Dirichlet or Neumann boundary condition at $\pm X$, then integration by parts would give the impossible statement that $v = 0$ on $[-X, X]$, finishing the proof:

$$0 = \text{Re} \int_{-X}^X \bar{v} \cdot P_\ell(\omega)v \, dx = -\text{Re}(v'\bar{v})\Big|_{-X}^X + \int_{-X}^X |v'|^2 + \text{Re}(\omega^2 V_1 + \ell(\ell+1)V_2)|v|^2 \, dx = 0,$$

and the terms under the integral are all nonnegative. This argument works also for v 's satisfying the defining properties of the QNM, as described below. For Kerr–de Sitter black holes a separation procedure is still possible but it does not work for stationary perturbations. Nevertheless in both cases the discreteness of QNM remains valid [24, 25].

To indicate how this works for resonant states which not satisfy a boundary condition at $\pm X$ (after all, this ‘boundary’ is completely artificial), we follow [20, §6]. It suffices to prove the boundary inequalities

$$\pm \text{Re}(v'(\pm X)\overline{v(\pm X)}) < 0. \quad (8)$$

To prove (8), we cannot use integration by parts on the whole \mathbb{R} , since v does not lie in $L^2(\mathbb{R})$ and moreover the real part of our potential may become negative as $x \rightarrow \pm\infty$. We instead use the methods of complex analysis and real analyticity of V_1, V_2 .

The characterization of v as a mode can be strengthened to say that $e^{\mp iV_\pm \omega x} v(x)$ is an *real analytic* function of $e^{-A_\pm |x|}$ (it has a convergent Taylor series in that variable), which means that for X large enough, we can extend $v(x)$ to a *holomorphic* function in $\{|\text{Re } z| \geq X\}$, and this extension is Floquet periodic: $v(z + 2\pi i/A_\pm) = e^{\mp 2\pi V_\pm \omega/A_\pm} v(z)$, $\pm \text{Re } z \geq X$. Now, consider the restriction of u to the vertical lines $\{\text{Re } z = \pm X\}$, $w_\pm(y) := v(\pm X + iy)$, $y \in \mathbb{R}$, and note that it solves the differential equation

$$(\partial_y^2 + \omega^2 V_1(\pm X + iy) + \ell(\ell+1)V_2(\pm X + iy))w_\pm = 0. \quad (9)$$

The key difference between (9) and the equation $P_\ell(\omega)v = 0$ is that the potential $V_2(\pm X + iy)$ is no longer real-valued. For instance, if V_2 were equal to $e^{-A_\pm |x|}$, then $V_2(\pm X + iy)$ would equal $e^{-X A_\pm} e^{\mp i A_\pm y}$, only taking real values when $y \in \pi A_\pm^{-1} \mathbb{Z}$. This means that the equation (9) is *elliptic* (in the semiclassical sense, where we treat ∂_y as having same order as ℓ) except at a discrete set of points in the phase space $T^*\mathbb{R}$. Further analysis shows that $w_\pm(y)$ is concentrated in phase space near $y \in 2\pi A_\pm^{-1} \mathbb{Z}$, $\eta = \mp \ell \sqrt{V_2(\pm X)}$, in particular implying

$$|(\partial_y \pm i\ell \sqrt{V_2(\pm X)})w_\pm(0)| \leq C\ell^{1/4}|w_\pm(0)|,$$

and (8) follows from Cauchy–Riemann equations, since $v(\pm X) = w_\pm(0)$ and $v'(\pm X) = -iw'_\pm(0)$.

IV. DISTRIBUTION OF QUASI-NORMAL MODES

The distribution of QNM ω_k can now be studied in the more general stable setting of r -normally hyperbolic trapped sets. Three fundamental issues are:

- (a) distribution of decay rates, that is of the imaginary parts of QNM;
- (b) asymptotics of the counting function;
- (c) expansion of waves in terms of QNM.

(a) We can bound the decay rates from below whenever the trapped set is normally hyperbolic, without requiring the stronger r -normal hyperbolicity assumption. The bound [33] is given by $\text{Im } \omega_k < -(\nu_{\min} - \varepsilon)/2$, for any $\varepsilon > 0$, once the frequency (the real part of ω_k) is large enough. In the case of r -normal hyperbolicity and under the pinching condition

$$\nu_{\max} < 2\nu_{\min}, \quad (10)$$

we get more detailed information [24]: there are additionally no QNM with

$$-(\nu_{\min} - \varepsilon) < \text{Im } \omega_k < -(\nu_{\max} + \varepsilon)/2. \quad (11)$$

That means that the modes with least decay are confined to a band shown in Fig.6. In the completely integrable case this follows from WKB constructions [20–23] – see Fig.6 – but this structure persists under perturbations. Fig.5 shows the accuracy of the estimate (11) for the numerically computed QNM of exact Kerr black holes [9]. For a recent experimental investigation of the distribution of decay rates and the relation to classical dynamics (more precisely, the topological pressure and classical escape rates) see [15].

The condition (10) is called pinching because it pinches the ratio of the maximal and the minimal transversal expansion rates. In the absence of this condition, the gap (11) between the first band of QNM and the faster decaying bands disappears, making it difficult to obtain a counting asymptotics (12). Physically, (10) could be interpreted as the requirement that there be no interaction between QNM from different bands.

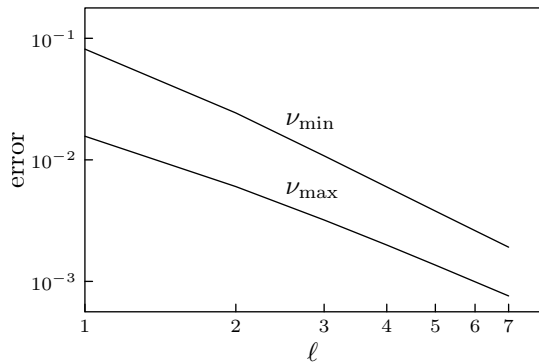


FIG. 5. A log-log plot of relative errors $\frac{|\min |\operatorname{Im} \omega_k(\ell) - \nu_{\min}/2|}{\min |\operatorname{Im} \omega_k(\ell)|}$ and $\frac{|\max |\operatorname{Im} \omega_k(\ell) - \nu_{\max}/2|}{\max |\operatorname{Im} \omega_k(\ell)|}$ where $\omega_k(\ell)$ are the numerically computed resonances in the first band corresponding to the angular momentum ℓ [9] and ν_{\min}, ν_{\max} are minimal and maximal expansion rates. The agreement is remarkable when ℓ increases.

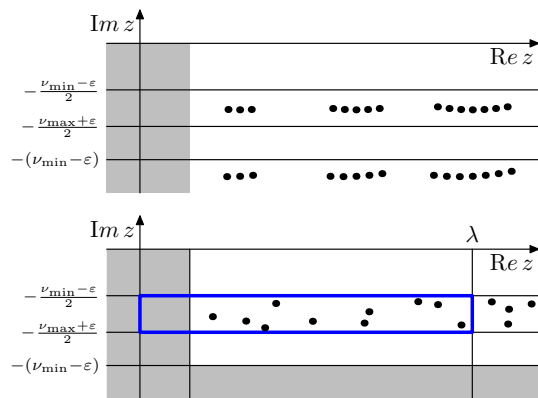


FIG. 6. A schematic comparison between QNM in a completely integrable case and in the general r -normally hyperbolic case. The former lie on a fuzzy lattice and are well approximated by WKB construction based on quantization conditions [20–23]. When trapping is r -normally hyperbolic and the pinching condition $\nu_{\max} < 2\nu_{\min}$ holds, quasi-normal modes are still localized to a strip with dynamically determined bounds, and their statistics are given by the Weyl law (12).

(b) The relation between the density of high energy states and phase space volumes defined by the classical Hamiltonian is one of the basic principles of quantum mechanics/spectral theory. It states that for closed systems the number, $N_{\hat{H}}(\lambda)$, of energy levels of \hat{H} , a quantization of H (for instance the Dirichlet Laplacian on a bounded domain), below energy λ^2 (we think of λ as frequency which is natural when considering QNM) satisfies the *Weyl law*

$$N_{\hat{H}}(\lambda) \sim (2\pi)^{-\dim X} \operatorname{vol}_{T^*X}(H \leq \lambda^2) \sim C_{\hat{H}} \lambda^{-\dim X}.$$

Here $\operatorname{vol}_{T^*X}$ denotes the phase space volume calculated using the volume $\sigma^{\dim X}/(\dim X)!$ obtained from the symplectic form σ (see (3)).

For open systems QNM replace real energy levels and the counting becomes much more tricky [14]. In the case of exact Kerr(–de Sitter) black holes the WKB constructions can be used to show that the number, $N_{\text{QNM}}(\lambda)$, of QNM with

$$|\omega_k| \leq \lambda, \quad \operatorname{Im} \omega_k \geq -(\nu_{\min} - \varepsilon)$$

satisfies the asymptotic law $N_{\text{QNM}}(\lambda) \sim c\lambda^2$. The constant c has a geometric interpretation: in a scattering problem the total phase space T^*X (the cotangent bundle of X) is replaced by the trapped set [34], and c corresponds to the symplectic volume of the trapped set.

The same law is proved [8] for perturbations of Kerr–de Sitter, using completely different ideas based on r -normal hyperbolicity rather than symmetries of the metric and separation of variables. Under the assumptions of r -normal hyperbolicity (4) and pinching (10), we have

$$N_{\text{QNM}}(\lambda) \sim \frac{\lambda^2}{(2\pi)^2} \operatorname{vol}(K \cap \{\xi_t^2 \leq 1\} \cap \{t = 0\}), \quad (12)$$

where the volume is taken using the symplectic form on $K \cap \{t = \text{const}\}$ [8, Thm 3]. We note that just as $\dim X = \frac{1}{2} \dim T^*X$ in the exponent of the Weyl law, here

$$2 = \frac{1}{2} \dim(K \cap \{t = \text{const}\}),$$

that is, the effective phase space is now the trapped set. For exact Kerr(–de Sitter) metrics with several values of Λ the volume as function of a is shown in Fig. 7. The volume is finite provided that $(1 - \Lambda a^2/3)^3 > 9\Lambda M^2$, see Fig. 1.

We should stress that normally hyperbolic behavior (unlike r -normal hyperbolicity) is often unstable under perturbations as shown by examples of hyperbolic quotients where a small perturbation can change the dimension of the trapped set [35, Fig.1], leading to a fractal Weyl law, that is a law in which the exponent 2 changes to half of the fractal dimension of the trapped set – see [14] for recent experiments on that.

(c) The expansion (6) is rigorously established for slowly rotating black holes [21, 31] and heuristically it is one of the motivations for studying quasi-normal modes [12]. For rapidly rotating black holes, or for their perturbations satisfying (10) a more robust version can be formulated using projector onto the states associated to quasi-normal modes in the first band shown in Fig. 6. The solution to the wave equation $\square_g u = 0$ with initial data localized near frequency $\lambda \gg 1$ can be decomposed as

$$u = u_{\text{QNM}} + u_{\text{DEC}}$$

where, for $0 \leq t \leq T \log \lambda$,

$$\square_g u_{\text{QNM}}(t), \quad \square_g u_{\text{DEC}}(t) = \mathcal{O}(\lambda^{-\infty}),$$

that is we have rapid decay (faster than any negative power) when the frequency λ is large. This means that

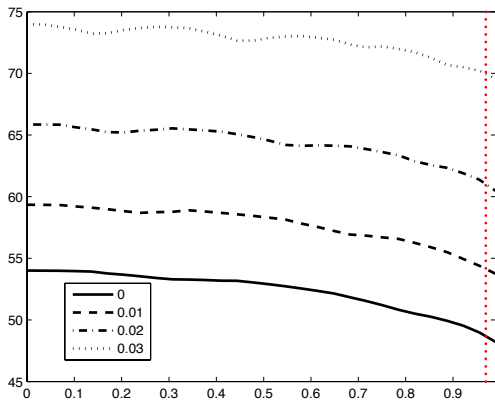


FIG. 7. Numerically computed constant in (12), $\text{vol}(K \cap \{\xi_t^2 \leq 1\} \cap \{t = 0\})/4\pi^2$, for $\Lambda = 0, 0.01, 0.02, 0.03$ and $M = 1$. The vertical line shows the value of a at which the pinching condition (10) fails for $\Lambda = 0$. For smaller values of a the Weyl law (12) holds. We note that as a increases the QNM split (see Fig. 6) and hence we do expect the counting function to decrease, in agreement with the behavior of the volume. From the volume and the gap giving the decay rate one can read off a and M .

both terms solve the wave equation approximately at high energies times bounded logarithmically in λ . We then have, again for $0 \leq t \leq T \log \lambda$,

$$\begin{aligned} \|u_{\text{QNM}}(t)\|_{\mathcal{E}} &\leq C e^{-(\nu_{\min} - \varepsilon)t/2} \|u_{\text{QNM}}(0)\|_{\mathcal{E}}, \\ \|u_{\text{QNM}}(t)\|_{\mathcal{E}} &\geq C^{-1} e^{-(\nu_{\max} + \varepsilon)t/2} \|u_{\text{QNM}}(0)\|_{\mathcal{E}}, \\ \|u_{\text{QNM}}(0)\|_{\mathcal{E}} &\leq C \sqrt{\lambda} \|u(0)\|_{\mathcal{E}}, \\ \|u_{\text{DEC}}(t)\|_{\mathcal{E}} &\leq C \lambda e^{-(\nu_{\min} - \varepsilon)t} \|u(0)\|_{\mathcal{E}}, \end{aligned} \quad (13)$$

where strictly speaking errors $\mathcal{O}(\lambda^{-\infty}) \|u(0)\|_{\mathcal{E}}$ should be added to the right hand sides. The norm $\|\cdot\|_{\mathcal{E}}$ is the standard energy norm in any sufficiently large compact subset of X (in the case of exact Kerr–de Sitter, we can take $(r_+ + \delta, r_C - \delta) \times \mathbb{S}^2$) – see [8, Thm 2]. The term $u_{\text{QNM}}(t)$ corresponds to the part of the solution dominated by the QNM in the first band and it has the natural decay properties dictated by the imaginary parts of these QNM. In fact, $u_{\text{QNM}}(t)$ can be physically interpreted as the radiation coming from light rays traveling along the

trapped set. The directions in which such a light ray radiates towards infinity can be described in terms of the geometry of the flow, and the amplitude of the radiated waves can be calculated using the global dynamics of the flow near the trapped set [24, §8.5].

V. CONCLUSIONS

We have shown that for Kerr–de Sitter metrics and their perturbations quasi-normal modes are rigorously defined and form a discrete set in the lower half plane, provided that the parameters of the black hole satisfy

$$(1 - \Lambda a^2/3)^3 > 9\Lambda M^2 > 0,$$

see Fig. 1. This is due to the size of infinity when $\Lambda > 0$ and the compactness of the trapped set at finite energies.

If one neglects the issues of long time decay and of behavior at low energies, then the results are also valid in the case of $\Lambda = 0$. On the length scales involved in the ringdown phenomenon, which in principle would lead to the detection of black hole parameters through QNM, the (small) value of Λ is not relevant but $\Lambda > 0$ is a more convenient mathematical model.

The main dynamical feature of the set on which photons are trapped (the trapped set) is its r -normal hyperbolicity for any r – see (4). Because of the stability of this property the main features of the distribution of quasi-normal modes are preserved for perturbations: the decay rates are bounded from below in terms of the minimal expansion rate ($\text{Im } \omega_k \leq -(\nu_{\min} - \varepsilon)/2$) and under the pinching conditions, the least decaying modes are confined to a strip where they satisfy a counting law (12) – see Fig. 6.

The r -normal hyperbolicity is valid for all rotating black holes but the pinching condition (10) needed for the finer results (12) and (13) fails in the case of very fast rotation – see Fig. 3.

ACKNOWLEDGMENTS. This work was partially supported by the National Science Foundation grant DMS-1201417 (SD,MZ) and by the Clay Research Fellowship (SD). We are grateful to Mihalis Dafermos for stimulating discussions of black hole physics and to Stéphane Nonnenmacher for comments on earlier versions of this note. We are also thankful to three anonymous referees for suggesting many improvements in the presentation.

[1] R.P. Kerr, Phys. Rev. Lett. **11**(5)(1963), 237–238.
[2] S. Perlmutter et al, ApJ **483**(1997), 565–581; A.G. Riess et al, AJ **116**(1998), 1009–1038.
[3] K.D. Kokkotas and B.G. Schmidt, Living Rev. Relativity **2**(1999).
[4] B. Carter, Phys. Rev. **174**(1968), 1559–1571.
[5] V.I. Arnold, Mathematical methods of classical mechanics, 2nd edition, Graduate Texts in Mathematics, 60.

Springer-Verlag, New York, 1989.
[6] M.W. Hirsch, C.C. Pugh, and M. Shub, “Invariant manifolds” Lecture notes in mathematics, **538**, Springer, 1977.
[7] J. Wunsch and M. Zworski, Ann. Inst. Henri Poincaré (A), **12**(2011), 1349–1385.
[8] S. Dyatlov, [arXiv:1305.1723](https://arxiv.org/abs/1305.1723)
[9] E. Berti, V. Cardoso, and A. Starinets, Class. Quant.

- Grav. 26(2009) 163001.
- [10] E. Berti et al. Phys. Rev. D **76**(2007), 064034.
- [11] M. Campanelli et al. Classical and Quantum Gravity **27**(2010), 084034.
- [12] E. Berti and K.D. Kokkotas, Phys. Rev. D 71(2005) 124008; G.T. Horowitz and V.E. Hubeny, Phys. Rev. D 62(2000) 024027, R.A. Konoplya and A. Zhidenko, Rev. Mod. Phys. 83, 793–836 (2011).
- [13] M. Zworski, Notices of Amer. Math. Soc. **46**(3), 319–328.
- [14] A. Potzuweit, T. Weich, S. Barkhofen, U. Kuhl, H.-J. Stöckmann and M. Zworski, Phys. Rev. E. 86, 066205 (2012).
- [15] S. Barkhofen, T. Weich, A. Potzuweit, U. Kuhl, H.-J. Stöckmann and M. Zworski, Phys. Rev. Lett. 110, 164102 (2013).
- [16] S. Iyer and C. M. Will, Phys. Rev. D 35, 3621–3631 (1987).
- [17] F. Fernández-Alonso and R.N. Zare, Annu. Rev. Phys. Chem. 2002. 53:67–99
- [18] A. Sá Barreto and M. Zworski, Math. Res. Lett. **4**(1997), 103–121;
- [19] H. Beyer, Comm. Math. Phys. **204**(1999), 397–423.
- [20] S. Dyatlov, Comm. Math. Phys. **306**(2011), 119–163
- [21] S. Dyatlov; Ann. Inst. Henri Poincaré (A), **13**(2012), 1101–1166.
- [22] S. Hod, Phys. Rev. D 75:064013 (2007); Phys. Rev. D 78:084035 (2008); Phys. Let. B 715, **348**(2012).
- [23] H. Yang, D. Nichols, F. Zhang, A. Zimmerman, Z. Zhang, and Y. Chen, Phys. Rev. D **86**(2012), 104006; H. Yang, F. Zhang, A. Zimmerman, D. Nichols, E. Berti, and Y. Chen, Phys. Rev. D **87**(2013), 041502.
- [24] S. Dyatlov, [arXiv:1301.5633](#).
- [25] A. Vasy, Inv. Math. 2013. [arXiv:1012.4391](#).
- [26] A. Goussev, R. Schubert, H. Waalkens, and S. Wiggins, Adv. Quant. Chem. **60**(2010), 269–332.
- [27] R.H. Price, Phys. Rev. D (3), 5:24192438, 1972.
- [28] M. Dafermos and I. Rodnianski, Invent. Math. **162** (2005), 381–457; R. Donniger, W. Schlag, A Soffer, Comm. Math. Phys. **309** (2012), 51–86; D. Tataru, Amer. J. Math. **135** (2013), 361–401.
- [29] S. Dyatlov, Math. Res. Lett. **18**(2011), 1023–1035.
- [30] S. Akcay and R.A. Matzner. Classical and Quantum Gravity **28.8**(2011), 085012.
- [31] J.-F. Bony and D. Häfner, Comm.Math.Phys. **282**(2008), 697–719.
- [32] A. Bachelot and A. Motet-Bachelot. Ann. Inst. H. Poincaré Phys. Théor. 59.1 (1993), 3–68.
- [33] S. Nonnemacher and M. Zworski, [arXiv:1302.4483](#).
- [34] J. Sjöstrand, Duke Math. J., 60, 1 (1990); W. T. Lu, S. Sridhar, and M. Zworski, Phys. Rev. Lett 91, 154101 (2003); J. Sjöstrand and M. Zworski, Duke Math. J., 137, 381 (2007).
- [35] K. Datchev and S. Dyatlov, Geom. Funct. Anal. 23, 1145–1206 (2013).